

Research Article

Reflectometric System for Continuous and Automated Monitoring of Irrigation in Agriculture

Egidio De Benedetto ^{1,2}, Giuseppe Cannazza,¹ Antonio Masciullo,¹
Christian Demitri ¹ and Andrea Cataldo ¹

¹Department of Engineering for Innovation, University of Salento, Lecce 73100, Italy

²MoniTech srl, 73100 Lecce, Italy

Correspondence should be addressed to Egidio De Benedetto; egidio.debenedetto@unisalento.it

Received 20 June 2018; Accepted 29 October 2018; Published 7 November 2018

Academic Editor: Ayman Suleiman

Copyright © 2018 Egidio De Benedetto et al. This is an open access article distributed under the Creative Commons Attribution License, which permits unrestricted use, distribution, and reproduction in any medium, provided the original work is properly cited.

In this work, a time domain reflectometry (TDR)-based system for continuous and diffused monitoring of soil water content in agriculture is presented. The proposed TDR-based system employs elongate sensing elements (SEs). In practical application, each wire-like SE is buried along the cultivation row to be monitored, and through a single TDR measurement it is possible to retrieve the water content profile of the cultivation along the length of the SE. By connecting the TDR-based monitoring system to the irrigation machines, it would be possible to automatically start/stop irrigation based on the actual water requirement of the cultivations, thus favoring precision agriculture and enhancing irrigation efficiency. To demonstrate the feasibility of the proposed monitoring solution, a dedicated hardware+software platform was developed and the TDR-based system was experimented in open-field cultivations.

1. Introduction

Irrigation is crucial in the economic and productive management of agricultural systems; as a result, the efficiency of water use has become a priority also due to the increasing limitations on this natural resource [1]. To mitigate this problem, it is necessary to develop technologies and practices that can provide effective solutions, but that can still be accessible (in terms of costs and easiness of use) to farmers [2]. Recently, precision irrigation technologies have been considered as a potential strategy to improve crop productivity under conditions of increasing water scarcity [3]. Also, the application of machine learning on sensor data has been considered for providing farmers with predicting irrigation recommendations [4].

Appropriately designed and built irrigation systems are essential for optimizing the irrigation process, increasing cultivation profitability, rationalizing available resources, and reducing waste. In such a scenario, the automated and real-time monitoring of the actual water requirement is strategic for the optimal management of agricultural systems.

The first step for assessing the cultivation's water requirement is to assess soil moisture content. However, at the state of the art, soil moisture content sensors are usually point sensors; therefore, a large number of point sensors would be required to monitor extended cultivation areas. This ends up limiting the possibility of real-time monitoring, and automated irrigation control can only rely (at best) on preestablished irrigation scheduling or on weather stations.

In such a context, the objective of this work was to develop and validate an innovative system based on the use of time domain reflectometry (TDR) technique and of elongate, low-cost sensing elements (SEs) for continuous and real-time, diffused monitoring of soil water content. The SEs are buried in the soil, close to the cultivations to be monitored. One single SE could be tens of meters long and would allow assessing the water content profile of the cultivation.

The developed monitoring system would communicate with the irrigation systems, and it would be able to control the valves automatically, depending on the water content detected in the soil, possibly allowing limiting irrigation only to the zones in need of water. In practical applications,

when the measured soil moisture content falls below an alert threshold, the system would open the automatic control valves, thus starting irrigation. Similarly, in the case of excessive water content in the soil (for example, because of rain), the system would prevent the start of the pumping system, thus delaying irrigation. The proposed system can encompass the three major components of a sustainable agricultural management as identified in [5], namely, real-time monitoring, decision-making, and remote access.

In the following, first, the background is briefly outlined. Successively, the materials, the methods, and the developed hardware/software platforms are described in detail. Then, the results of the experimental validation of the system in two practical application scenarios are reported (one set of experiment relates to a cultivation of trees and the other relates to plant cultivation). Finally, results are discussed and conclusions are drawn.

TDR is a well-established measurement technique used in several fields. This technique has low implementation costs and offers the possibility of remote control and continuous monitoring. Additional features such as real-time response and adaptability make TDR particularly attractive for countless applications (e.g., localization of wire faults [6–8], liquid level monitoring [9], dielectric characterization of materials [10–12], monitoring building structures [13], quality control on vegetable oils [14], landslide and ground movement monitoring [15, 16], leak detection in underground pipes [17], etc.)

The literature related to TDR-based soil moisture content measurements is extensive [18–22]; however, traditional TDR soil moisture content measurements rely on short, multirod probes for local moisture content measurements. On the other hand, the monitoring system described herein relies on elongate SEs, similar to the ones employed for the localization of leaks in underground pipes [23] and for monitoring building structures [24, 25].

TDR relies on the analysis of the signal that is reflected when an electromagnetic signal (typically, a voltage step signal with very fast rise time or a pulse signal) is propagated along a probe or a SE inserted into the system under test. In particular, the propagating TDR signal is reflected at the electrical impedance variations encountered along its path [26].

The typical output of a TDR measurement is a reflectogram, which displays the reflection coefficient (ρ) of the system under test as a function of the apparent distance (d^{app}).

As a general rule, the higher the relative dielectric permittivity of the medium in which the SE is inserted, the slower will the TDR signal propagate along the SE [27]. This means that the distance travelled by the TDR signal will “appear” longer than the physical distance actually travelled (d), according to the following equation:

$$d^{app} = \sqrt{\epsilon^{app}} \cdot d \quad (1)$$

where (d^{app}) is the apparent/electrical distance and ϵ^{app} is referred to as apparent dielectric constant of the medium in which the signal propagates.

With regard to ρ , this quantity is related to the variations of relative dielectric permittivity encountered by the propagating TDR signal. A constant value of ρ means that the dielectric characteristics in that portion of path are uniform. Vice versa, variations of ρ in the reflectogram indicate that the dielectric characteristics change along the travelled electrical path (as detailed later, depending on the internal architecture of the TDR instrument, a different quantity may be present in place of ρ).

On such basis, the proposed TDR-based system relies on sensing the variations of the dielectric permittivity that occur in the soil as a result of irrigation. In fact, the relative dielectric permittivity of water is approximately 78 [28], while the relative dielectric permittivity of dry soil is usually in the range 3-10 (depending on the type of soil). When the soil is moistened with water, the dielectric permittivity of the moist soil will increase. In particular, the higher the water content, the higher will be the increase of dielectric permittivity. In the output reflectogram, an increase of soil dielectric permittivity will appear as a drop of ρ (typically, a dip of the reflectogram) [26]. By identifying the abscissa where this dip occurs, it can also be possible to localize the zone where the soil is wetter.

2. Materials and Methods

Two major sets of experiments were carried out for validating the proposed system:

- (i) soil water content measurements in a cultivation of trees;
- (ii) soil water content measurements in plant cultivations.

In the following sections, the materials and methods used in these experiments are described in detail.

2.1. Description of the TDR Monitoring System. For the diffused soil moisture measurements, the TDR-307usb instrument was used. This instrument was selected because of the optimal trade-off between measurement accuracy and low cost (approximately 1'000 Euros); hence, it is ideal for agricultural applications which are generally characterized by stringent cost requirements. The TDR-307usb is a portable instrument that generates a pulse signal, whose duration can be varied from 10 ns to 50 μ S. This instrument has rugged on-board electronics, and it is powered directly through the USB port of the laptop.

As for the elongate SE, the sensing section consists of an RG59 coaxial cable and of a wire (W1), which are mutually insulated and run parallel to each other. Figure 1 shows the schematisation of the axonometric cross section. In the coaxial cable, the inner conductor is made of copper and has a diameter of 1.6 mm; the insulator is made of polyethylene and has a diameter of 7.1 mm; the shielding outer conductor is a copper foil; finally, the protective plastic covering is made of PE and has a diameter of 15 mm. As for W1, the wire is made of copper and it has a diameter of approximately 2 mm.

The coaxial cable serves only the purpose of calibrating the distance. In fact, first the TDR signal is propagated along the coaxial cable to assess the actual length of the

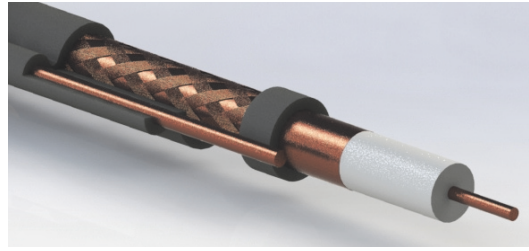


FIGURE 1: Axonometric cross section of the elongate SE. A copper wire runs parallel to a coaxial cable.

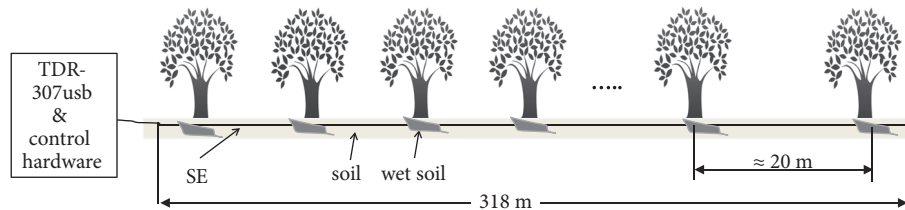


FIGURE 2: Experiment #1: schematization of the disposition of the SE along the row of trees. The trees were approximately 20 m apart. Dimensions not to scale.

sensing section (in this way, the SE can be cut according to the cultivation length, without preliminarily establishing the length of the SE).

Instead, the SE itself consists of the bifilar transmission line that is formed by two elongate conductors: the outer conductor of the RG59 and the wire W1.

2.2. Development of the Control Hardware and Software for the Practical Use of the Monitoring System. For the practical use of the proposed system, also a dedicated hardware platform for controlling the irrigation system was implemented. The core of the hardware platform consists of the TDR RI-307usb, a Raspberry Pi, a relay module (SMTRELAY08), and electrovalves. The hardware platform also includes the necessary peripherals, namely, a touchscreen monitor display, a 2A 5V power supply, and a memory card.

As for the developed software, in addition to acquiring and storing the measurement data, the developed software can control the valves of the irrigation system, according to the measured value of soil water content. The operating system chosen for the software is Raspbian Stretch with desktop version: the programming language chosen to write the algorithm was Python 3. The software allows

- (i) selecting a distance range in which to check soil water content;
- (ii) setting soil water content thresholds, in correspondence of which the valves are to be opened/closed.

With regard to the output of the monitoring system, specific data are provided in the experimental section. However, it is useful to describe the behaviour of the typical output. By default, the abscissa axis reports the apparent distance (d^{app}); however, through an appropriate calibration, the actual physical distance (d) can be displayed.

As for the ordinate axis, in the previous section it was mentioned that typically the reflection coefficient (ρ) is displayed. Indeed, depending on the internal architecture of the TDR instrument, a different quantity may be present in place of ρ . This may be the reflected voltage, the electrical impedance, or any other quantity related to the reflected signal. The used TDR RI-307usb instrument provides a dimensionless quantity (K), which is a proportionality coefficient between the reflected TDR signal and the reference used by the A/D converter of the TDR instrument. Clearly, the behaviour of K is strictly related to the reflection coefficient.

2.3. Description of the Setup for Experiment #1. In the first set of experiments, a tree cultivation was considered. The separation between the trees was approximately 20 m. A SE with length 318 m was placed along the row of trees, as depicted in Figure 2. The cultivation was equipped with emitters for drip irrigation. Before and after irrigation, the SE was connected to the TDR RI-307usb and was interrogated through the developed hardware and software platform.

2.4. Description of the Setup for Experiment #2. Also this experiment was carried out in an open-field cultivation. In particular, 12 SEs were positioned along as many rows of plants; the length of each elongate SE was $L_{SE} = 35$ m. The SEs were buried approximately 20 cm underground. Figure 3 shows a sketch of the experimental setup. The letters b and e indicate the beginning and the end of each elongate SE.

For the TDR measurements, the TDR-307usb was connected to the beginning of each SE, thus obtaining one reflectogram for each plant row.

In addition to the elongate SEs, also eight two-rod probes (v_1, \dots, v_8) were inserted vertically inside the soil, in correspondence of eight measurement points indicated in Figure 3(a). This was done to have a local countercheck of soil

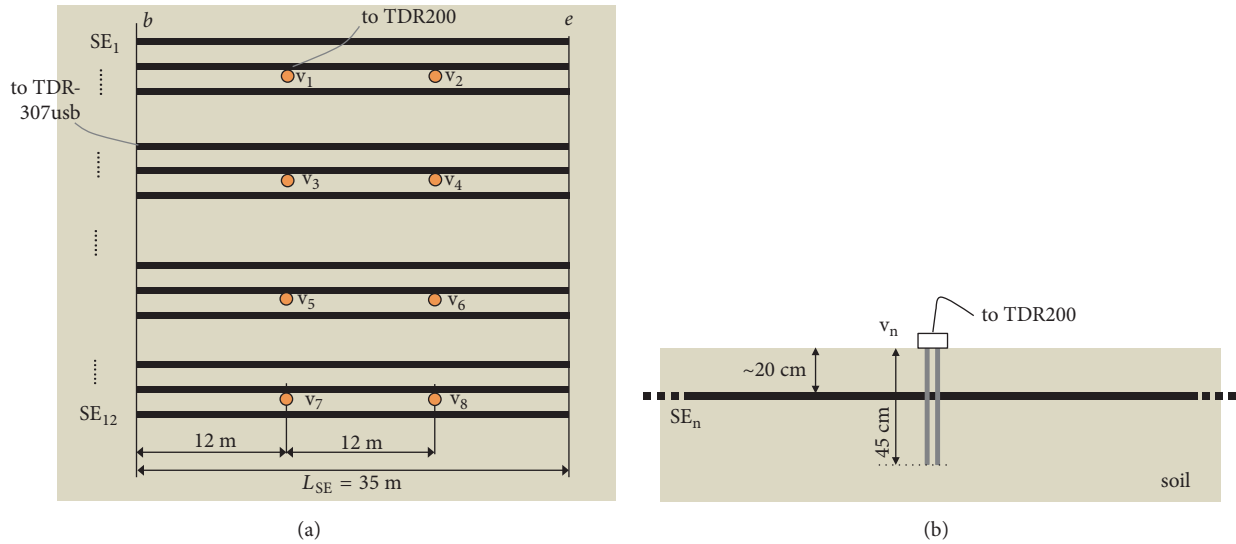


FIGURE 3: Experiment #2: (a) top-view schematization of the experimental setup. SE₁, ..., SE₁₂ indicated the sensing element. v₁, ..., v₈ indicate the vertical local probes. (b) Longitudinal section in correspondence of one of the SEs. Dimensions not to scale.

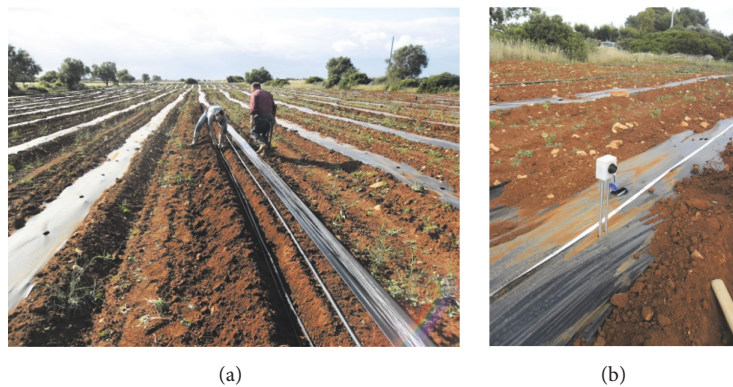


FIGURE 4: Experiment #2: (a) picture of the arrangement of the elongate SEs. (b) Picture of one of the vertical probes.

water content. Each vertical probe was made of two 45 cm long parallel rods (diameter 6 mm) made of stainless steel. A teflon block keeps the rod parallel and mechanically stable and it also contains the electrical connector for connecting the TDR instrument.

Figure 3(b) shows a longitudinal section in correspondence of one of the elongate SEs. It can be seen that the vertical probe is fully inserted in the soil.

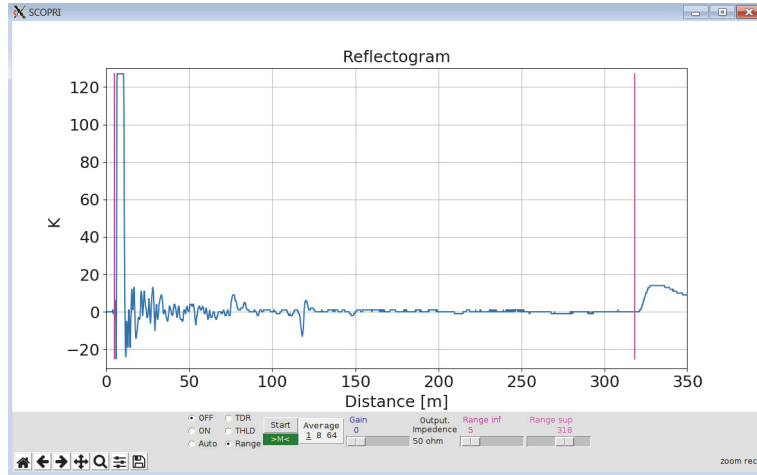
Figures 4(a) and 4(b) show a picture of the arrangement of one of the elongate SEs and of one of the vertical probes, respectively.

It is important to point out that the TDR measurements with the vertical probes were carried out through the TDR200 reflectometer. This portable instrument generates a step-like signal with fast rise time. This TDR instrument includes a more sophisticated electronic; hence, the cost of the TDR200 is approximately 5'000 Euros. Although the cost of this piece of equipment is higher, it has the advantage that it can be connected to multiplexers and can control up to 512 SEs, thus reducing considerably the implementation costs.

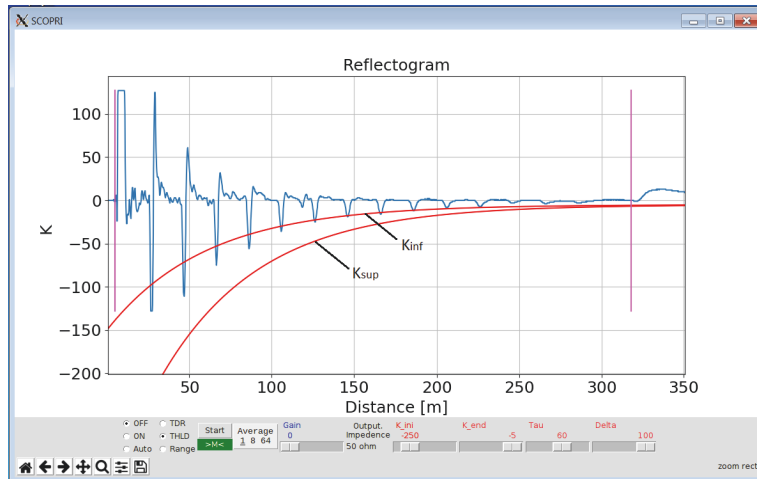
3. Experimental Validation of the System: Results and Discussion

3.1. *Experiment #1.* After positioning the elongate SE as depicted in Figure 2, a reflectogram was acquired before irrigation (Figure 5(a)). The abscissa was calibrated in terms of actual distance. The first peak in the reflectogram corresponds to the incident TDR signal. The vertical markers in the figure indicate the abscissae corresponding to the beginning and the end of the SE. The peak at approximately $d = 318$ m corresponds to the end of the SE. It can be seen that, in dry condition, the value of K appears generally constant as a result of the fact that the relative dielectric permittivity of the dry soil is practically homogeneous.

Successively, the trees were drip-irrigated for several hours. After irrigation, another reflectogram was acquired (Figure 5(b)). The addition of water in correspondence of the trees led to a local increase of the relative dielectric permittivity of the soil. As a result, the appearance of several



(a)



(b)

FIGURE 5: Experiment #1: (a) reflectogram acquired in dry condition; (b) reflectogram acquired after drip irrigation. The threshold curves for K are also indicated.

minima points of K in correspondence of the position of the trees can be noticed.

It can be observed that although the same amount of water (approximately 50 litres) was provided to each tree, the peaks are less prominent as the distance increases. This is due to the attenuation of the propagating TDR electromagnetic signal along the 318 m long SE.

Because of electromagnetic losses, minima at difference distance d (for example, one at shorter distance along the SE and another at farther distance along the SE) may exhibit a different amplitude, even when the soil water content is the same. In particular, it is observed that the minima of K appear to follow the trend of an exponential curve which can be described as

$$K = K_{\infty} + (K_0 - K_{\infty}) \cdot \exp\left(-\frac{d}{\tau}\right) \quad (2)$$

where K_{∞} , K_0 , and τ are the fitting coefficients. Indeed, the fitting curve (not reported here for brevity) resembles the

typical behaviour of the attenuation coefficient, which is the attenuation of an electromagnetic wave propagating through a medium per unit distance from the source [29]. Clearly, for higher-quality (more costly) SEs, losses are lower and the amplitude of the minima would be less dependent on the distance.

As mentioned in Section 2.3, the developed software allows setting the thresholds for K , following the observed exponential behaviour. The exponential marker curves in Figure 5(b) indicate the optimal K -range. Clearly, also the thresholds (K_{inf} and K_{sup}) must take into account the effect of electromagnetic losses, in order to compensate for them. In this way, through a simple in-the-field calibration, the operator could establish empirically the relationship between an optimal reference percentage of water for the specific soil and cultivation and the distance. These marker curves must be identified for the specific cultivation and soil. These input data can be stored in the control software and used for an automatic optimization of irrigation.

The thresholds K_{inf} and K_{sup} are used “dynamically” with respect to how soil water changes in time. If a reflection (i.e., a dip in the reflectogram) is above the threshold set by the K_{inf} marker, then the TDR monitoring system senses that the cultivation needs water and starts the irrigation of the soil. The TDR monitoring systems regularly acquires updated reflectogram. The irrigation process continues until, in the automatically-updated reflectogram, the value of K falls below K_{sup} .

On the other hand, if the dip is lower than K_{sup} (for example, because of rainy water), then the monitoring system senses that there is an excess of water content and irrigation is prevented.

When the dip rises up to and (again) higher than K_{inf} , then irrigation starts. Irrigation is stopped when in the updated reflectogram the dip decreases to K_{sup} .

This cycle repeats throughout the cultivation lifetime. This procedure allows maintaining the desired amount of soil water content, thus satisfying the cultivation water requirement.

3.2. Experiment #2. In the second set of experiments, the arrangement of the SEs was as depicted in Figure 3. TDR measurements were carried out in the following days and conditions:

- (i) Day #1: approximately one week after seeding to make sure that the soil was settled;
- (ii) Day #14: one hour after 3.5 h long irrigation;
- (iii) Day #20: before irrigation;
- (iv) Day #21: approx. 10 hours after a 3.5 h long irrigation;
- (v) Day #24: before irrigation.

For the sake of brevity only the results related to one of the elongate SEs are reported. In particular, Figure 6 shows a comparison of the reflectograms acquired from one of the SEs (namely, SE₃) during the observation period. However, the results obtained from the other SEs were consistent.

- (i) Day #1: in this condition, the soil was dry. From the reflectogram, at approximately $d^{app} = 10$ m, the typical peak associated with the incident TDR signal can be noticed. The beginning of the SE is at approximately $d^{app} = 17.8$ m, while the end of the SE falls at approximately $d^{app} = 78.4$ m. The subsequent peak is, in fact, the typical signature associated with the open-ended termination of the SE. It can be noticed that the portion of the reflectogram corresponding to the SE is practically constant. This means that the relative dielectric permittivity of the dry soil is homogeneous.
- (ii) Day #14: the plants were irrigated for 3.5 h. The TDR measurement was carried out after waiting approximately one hour, in order to allow water to diffuse and settle. It can be seen that while the d_B^{app} has remained the same, the value of d_E^{app} has increased up to 97.1 m. The lengthening of the apparent length of the SE is a direct result of the overall increase of the dielectric permittivity of the moistened soil,

in accordance with (1). It can also be noticed that the value of K is constant along the SE. This means that there is no significant variation of the dielectric permittivity of the soil along the SE; hence, the water diffused homogeneously in the soil along the SE.

- (iii) Day #20: one day before the scheduled irrigation, another TDR measurement was carried out. From the reflectogram, it can be seen that d_E^{app} has decreased at approximately 90.2 m, thus resulting in an overall decrease of the apparent length of the SE. This indicated that the soil has dried up. Also in this case, the soil moisture content seems homogenous along the SE, as can be deduced from the flatness of the curve.
- (iv) Day #21: the irrigation went on for 3.5 h, and after waiting an additional ten hours, another reflectogram was acquired. As expected, because of the irrigation, the apparent length of the SE has increased, as d_E^{app} shifted up to 95.1 m.
- (v) Day #24: one day after irrigation, another TDR measurement was performed. Once again, the apparent length of the SE has decreased ($d_E^{app} \cong 91.3$ m).

The observation lasted for approximately three months, for the whole lifetime of the cultivations. The trend of the lengthening/shortening of the apparent length of the SE was confirmed throughout the observation period. The behaviour was consistent with all the 12 SEs.

It should be mentioned that, from these measurements, it was not possible to discriminate zones with higher moisture content. This is due to the fact that the mutual distance between the plants was approximately 30 cm, and as a result of the irrigation the water diffused also in between the plants. However, the lengthening of the apparent length of SE was a consistent indicator of the variation of soil moisture content.

For the sake of example, Figure 7 shows the reflectograms acquired from probe v_1 . In the figure, the abscissae corresponding to the beginning and to the end points of the vertical probe are indicated. It can be seen that, throughout the observation period, there is a very little variation in the apparent length of the probe. Therefore, if we were to use (1) to determine soil moisture content from the vertical probe, the result would be that the relative dielectric constant did not change considerably during the observation period. In other words, based on the vertical probe results, one should conclude that the soil was always wet. This is due to the fact that the “traditional” vertical probe provides an overall value of the moisture content along its length. Because the water provided to the plants saturated the superficial layer of soil and diffused beneath, the vertical probe senses the overall presence of water content. Nevertheless, this water was not available to the plant roots, but had diffused below.

4. Considerations on Practical Applications

In view of possible application of the proposed system, it is important to make some considerations regarding the implementation costs and modalities.

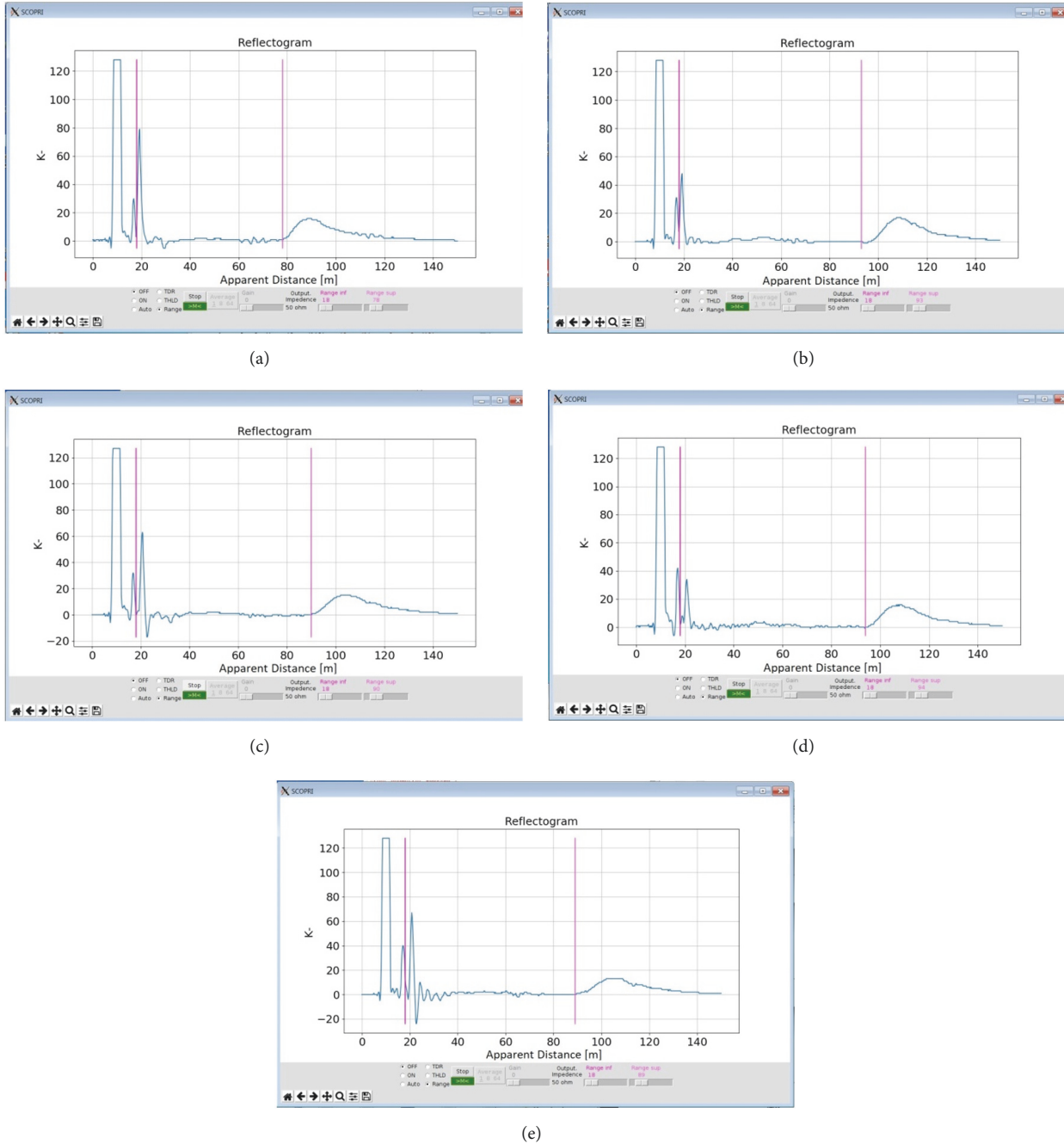


FIGURE 6: Experiment #2: comparison of the reflectogram acquired from SE₃ during the observation period: (a) day #1; (b) day #14; (c) day #20; (d) day #21; (e) day #24. The shift of the abscissa corresponding to the end of the SE indicates a different amount of soil water content.

With regard to the cost of the SE, it may vary from approx. 0.20 €/m to 7 €/m, depending on the quality of the SE (in terms of internal losses, reusability, robustness, and durability in time) as required for the specific application. For example, for seasonal cultivations, it may be advisable to employ low-cost disposable SEs, which are used for a season and are then removed from the soil and disposed of. For monitoring cultivations of trees, on the other hand, more robust and durable (and costly) SEs could be used. In fact, in this case,

the lifetime of the SE is supposed to be comparable with that of the tree.

With regard to the TDR measurement instrument, as aforementioned, with some TDR instruments (as the TDR 200), it is possible to employ multiplexing devices. These allow controlling up to 512 SEs with a single measurement instrument, thus considerably reducing the implementation costs. Figure 8 shows a sketch of the possible configuration of a multiplexed TDR-based monitoring system.

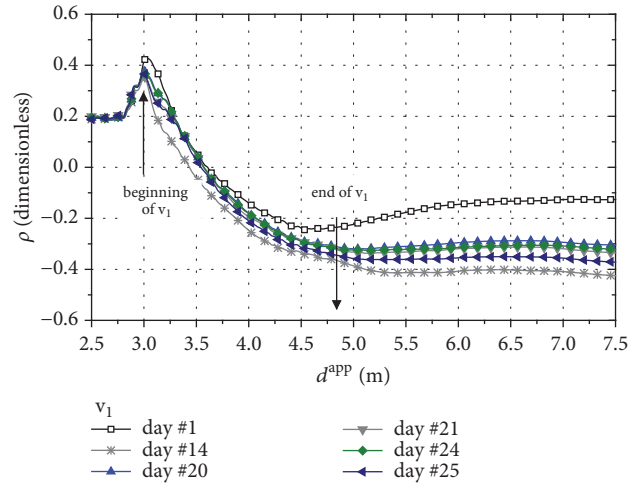


FIGURE 7: Experiment #2: reflectograms acquired from the vertical two-rod probe, v_1 .

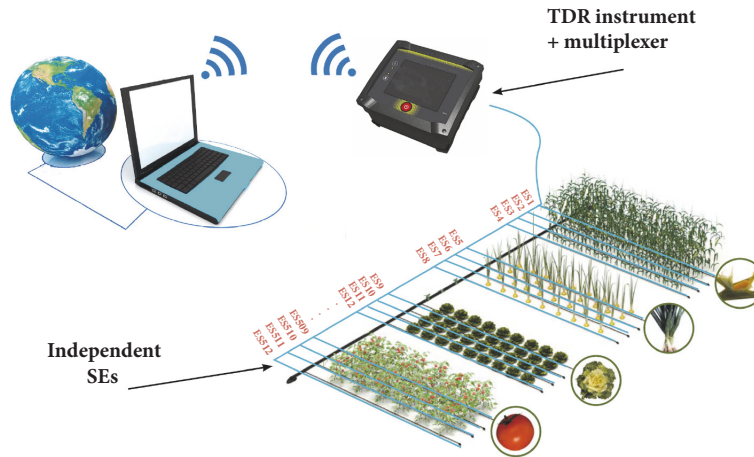


FIGURE 8: Sketch of the possible configuration of the system for monitoring, with a single measurement instrument, up to 512 independent SEs.

As for the installation of the SE, it consists only in burying the SE approximately 10-50 cm underground (depending on the cultivation). The procedure is very simple and only requires letting one end of the SE emerge from the soil, in order to allow the connection to the measuring instrument.

Finally, with regard to the “density” of installation of SEs (i.e., number of SEs per ha), thanks to the modularity of the proposed system, it follows that a high degree of freedom is available. Based on the experimental validation carried out so far, large farms could be entirely monitored with hundreds of SEs; however, the farmer could choose to monitor the moisture content profile on selected zones in the cultivations. The operator may as well choose not to install a SE along each row, but, for example, one SE every 0.5 ha. In the experience of the authors so far, for a given cultivation, an optimal trade-off for the density of installation may be one SE every 10-15 rows. And, if multiple cultivations are present, then the aforementioned procedure should be followed for each cultivation.

5. Conclusions

In this work, a TDR-based system for continuous and diffused monitoring of soil water content in agriculture was presented. Differently from traditional point sensors, the proposed system allows monitoring the soil water content profile along elongate SEs buried along the cultivation rows. The suitability of the developed TDR-based system for the intended application was tested in actual open-field cultivations.

The proposed system holds considerable potential as a cost-effective solution for real-time monitoring of soil water content in agriculture. In practical applications, by connecting the proposed measurement system to the irrigation machines, it would be possible to automatically start/stop irrigation based on the actual water requirement of the cultivations. This integration of the proposed system with irrigation systems could favor precision agriculture and enhancing irrigation efficiency.

Data Availability

The data used to support the findings of this study are available from the corresponding author upon request.

Conflicts of Interest

The authors declare that there are no conflicts of interest regarding the publication of this paper.

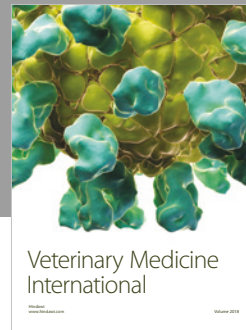
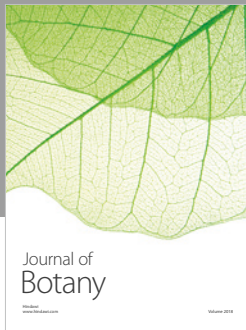
Acknowledgments

This research was funded by Regione Puglia-Area Politiche per lo Sviluppo Rurale-Servizio Agricoltura within the Public Notice “Call for Project Proposals for Research and Experimentation in Agriculture,” as part of the activities of the research project “SCOPRI - Sistema per il Controllo ed Ottimizzazione dei Processi di Irrigazione” (Eng.: “System for Control and Optimization of Processes of Irrigation”, project ID number: PRS 100). The paper reflects the authors’ point of view and not Regione Puglia’s.

References

- [1] J. F. Velasco-Muñoz, J. A. Aznar-Sánchez, L. J. Belmonte-Ureña, and M. J. López-Serrano, “Advances in Water Use Efficiency in Agriculture: A Bibliometric Analysis,” *Water*, vol. 10, no. 4, p. 377, 2018.
- [2] J. Pretty, “Agricultural sustainability: Concepts, principles and evidence,” *Philosophical Transactions of the Royal Society B: Biological Sciences*, vol. 363, no. 1491, pp. 447–465, 2008.
- [3] R. González Perea, A. Daccache, J. A. Rodríguez Díaz, E. Camacho Poyato, and J. W. Knox, “Modelling impacts of precision irrigation on crop yield and in-field water management,” *Precision Agriculture*, vol. 19, no. 3, pp. 497–512, 2018.
- [4] A. Goldstein, L. Fink, A. Meitin, S. Bohadana, O. Lutenberg, and G. Ravid, “Applying machine learning on sensor data for irrigation recommendations: revealing the agronomist’s tacit knowledge,” *Precision Agriculture*, vol. 19, no. 3, pp. 421–444, 2018.
- [5] Y. Lin, T. Chang, C. Fan et al., “Applications of Information and Communication Technology for Improvements of Water and Soil Monitoring and Assessments in Agricultural Areas—A Case Study in the Taoyuan Irrigation District,” *Environments*, vol. 4, no. 1, pp. 1–12, 2017.
- [6] C. Furse, Y. Chung, C. Lo, and P. Pendayala, “A critical comparison of reflectometry methods for location of wiring faults,” *Smart Structures and Systems*, vol. 2, no. 1, pp. 25–46, 2006.
- [7] C. Parkey, C. Hughes, and N. Locken, “Analyzing artifacts in the time domain waveform to locate wire faults,” *IEEE Instrumentation & Measurement Magazine*, vol. 15, no. 4, pp. 16–21, 2012.
- [8] O. Hoseini Izadi and D. Pommerenke, “Measurement of Dielectric Constant and Cross-Sectional Variations of a Wire,” *IEEE Transactions on Instrumentation and Measurement*, vol. 67, no. 6, pp. 1409–1416, 2018.
- [9] A. Thomsen, B. Hansen, and K. Schelde, “Application of TDR to water level measurement,” *Journal of Hydrology*, vol. 236, no. 3–4, pp. 252–258, 2000.
- [10] C.-P. Lin, S.-H. Tang, C.-H. Lin, and C.-C. Chung, “An improved modeling of TDR signal propagation for measuring complex dielectric permittivity,” *Journal of Earth Science*, vol. 26, no. 6, pp. 827–834, 2015.
- [11] X. Shuai, T. R. Green, and S. Logsdon, “Improved theory of time domain reflectometry with variable coaxial cable length for electrical conductivity measurements,” *Soil Science Society of America Journal*, vol. 81, no. 4, pp. 723–733, 2017.
- [12] C. Lin, Y. J. Ngui, and C. Lin, “Multiple Reflection Analysis of TDR Signal for Complex Dielectric Spectroscopy,” *IEEE Transactions on Instrumentation and Measurement*, vol. 67, no. 11, pp. 2649–2661, 2018.
- [13] A. Cataldo, E. De Benedetto, G. Cannazza, E. PiuZZi, and N. Giaquinto, “Embedded TDR wire-like sensing elements for monitoring applications,” *Measurement*, vol. 68, pp. 236–245, 2015.
- [14] L. Ragni, A. Berardinelli, C. Cevoli, and E. Valli, “Assessment of the water content in extra virgin olive oils by Time Domain Reflectometry (TDR) and Partial Least Squares (PLS) regression methods,” *Journal of Food Engineering*, vol. 111, no. 1, pp. 66–72, 2012.
- [15] L. Dengfeng, Z. Baowei, W. Gang, Y. Kebiao, W. Leiming, and X. Xuejie, “Time domain reflectometry calculation model of landslides slippage,” *Advances in Intelligent Systems and Computing*, vol. 455, pp. 327–336, 2017.
- [16] S. F. Aghda, K. Ganjalipour, and K. Nabiollahi, “Comparison of performance of inclinometer casing and TDR technique,” *Journal of Applied Geophysics*, vol. 150, pp. 182–194, 2018.
- [17] A. Cataldo, E. De Benedetto, G. Cannazza, C. Huebner, and D. Trebbels, “Performance comparison of TDR-based systems for permanent and diffused detection of water content and leaks,” *Measurement Science and Technology*, vol. 28, no. 1, 2017.
- [18] G. C. Topp, S. Zegelin, and I. White, “Impacts of the real and imaginary components of relative permittivity on time domain reflectometry measurements in soils,” *Soil Science Society of America Journal*, vol. 64, no. 4, pp. 1244–1252, 2000.
- [19] D. Moret, J. L. Arrúe, M. V. López, and R. Gracia, “A new TDR waveform analysis approach for soil moisture profiling using a single probe,” *Journal of Hydrology*, vol. 321, no. 1–4, pp. 163–172, 2006.
- [20] V. P. Drnevich, C. Zambrano, P.-T. Huang, and S. Jung, “TDR technologies for soil identification and properties,” *Geotechnical Special Publication*, vol. 175, p. 86, 2007.
- [21] S. I. Lee, D. G. Zollinger, and R. L. Lytton, “Determining moisture content of soil layers with time domain reflectometry and micromechanics,” *Transportation Research Record*, no. 2053, pp. 30–38, 2008.
- [22] W. Hong, Y. Jung, S. Kang, and J. Lee, “Estimation of Soil-Water Characteristic Curves in Multiple-Cycles Using Membrane and TDR System,” *Materials*, vol. 9, no. 12, pp. 1–15, 2016.
- [23] A. Cataldo, E. De Benedetto, G. Cannazza et al., “Recent advances in the TDR-based leak detection system for pipeline inspection,” *Measurement*, vol. 98, pp. 347–354, 2017.
- [24] A. Cataldo, E. De Benedetto, and G. Cannazza, “Hydration monitoring and moisture control of cement-based samples through embedded wire-like sensing elements,” *IEEE Sensors Journal*, vol. 15, no. 2, pp. 1208–1215, 2015.
- [25] A. Cataldo, E. De Benedetto, G. Cannazza, G. Monti, and E. PiuZZi, “TDR-based monitoring of rising damp through the embedding of wire-like sensing elements in building structures,” *Measurement*, vol. 98, pp. 355–360, 2017.

- [26] A. Cataldo and E. De Benedetto, "Broadband reflectometry for diagnostics and monitoring applications," *IEEE Sensors Journal*, vol. 11, no. 2, pp. 451–459, 2011.
- [27] M. H. Ali, "Water resources management," in *Practices of Irrigation & On-farm Water Management*, M. H. Ali, Ed., vol. 2, pp. 139–191, Springer Science, Amsterdam, Netherlands, 2011.
- [28] U. Kaatze, "Reference liquids for the calibration of dielectric sensors and measurement instruments," *Measurement Science and Technology*, vol. 18, no. 4, pp. 967–976, 2007.
- [29] R. Khurana, *Electromagnetic Field Theory*, Vika Publishing House, New Delhi, India, 2014.



Hindawi

Submit your manuscripts at
www.hindawi.com

